Isotopic and temperature effects on the photoemission and predissociation rates of $N_2^+(C\,^2\Sigma_u^+)$

C. Stemmle,[1] C. J. Villabona,[2] C. Forero,[2] B. Paulus,[1] and J. F. Pérez-Torres[2,*]

[1]*Freie Universität Berlin, Arnimallee 22, 14195 Berlin, Germany*

[2]*Universidad Industrial de Santander, Carrera 27 calle 9, Bucaramanga 680002, Colombia*

(Received 12 June 2020; accepted 12 August 2020; published 1 September 2020)

Radiative and nonradiative decay rates of the $C\,^2\Sigma_u^+$ electronic state of N_2^+ are calculated as a function of the temperature. This makes it possible to study the effect of the temperature on the photoemission spectrum and on the ion yields $I(N^+)$ and $I(N_2^+)$. It is shown that the temperature has different effects on the isotopes $^{28}N_2^+$, $^{29}N_2^+$, and $^{30}N_2^+$. Our results confirm that, regardless of the temperature, predissociation is the dominant relaxation mechanism for vibrational states $\nu' \geqslant 3$ of the $^{28}N_2^+$ and $^{29}N_2^+$ molecules.

DOI: 10.1103/PhysRevA.102.032802

I. INTRODUCTION

Early experiments on electron impact and collisions of He^+ ions with N_2 revealed a strong isotope effect on the radiative decay of the $N_2^+(C\,^2\Sigma_u^+ \rightarrow X\,^2\Sigma_g^+)$ molecular system [1–3]. This photoemission pathway is known as the second negative 2N system of N_2 [4,5]. Predissociation through an avoided crossing with the electronic state $B\,^2\Sigma_u^+$ comprises an alternative decay pathway of the $C^2\Sigma_u^+$ state [6–8], becoming a competitive and even, in some cases, the dominant mechanism, yielding a weakening of the photoemission signals and decreasing the lifetime of the vibrational levels [6]. The two unimolecular reactions can be described as

$$N_2^+(C^2\Sigma_u^+, \nu', J') \rightarrow N_2^+(X^2\Sigma_g^+, \nu'', J'') + \frac{hc}{\lambda} \quad (1)$$

$$\rightarrow N_2^+(B^2\Sigma_u^+, J'') \rightarrow N(^4S) + N^+(^3P), \quad (2)$$

where reaction (1) is constrained by the radiative selection rule $J'' = J' \pm 1$, while reaction (2) is constrained by the Kronig's selection rulres [9] $J'' = J'$, $E^{C}_{\nu' J'} = E^{B}_{J'}$ and occurs only for $\nu' \geqslant 3$. These two competing reactions, schematically illustrated in Fig. 1, proceed according to the photoemission $A^{em}_{\nu' J'}$ and predissociation $A^{pred}_{\nu' J'}$ rates. Two experimental methods have been employed to determine the vibrational resolved predissociation/photoemission ratios which characterize the 2N system of N_2. One method is based on the mass spectrometric measurements of the ion yields $I_{\nu'}(N^+)$ and $I_{\nu'}(N_2^+)$, from which the predissociation/photoemission ratios can be obtained as $A^{pred}_{\nu'}/A^{em}_{\nu'} = I_{\nu'}(N^+)/I_{\nu'}(N_2^+)$ [2,10]. The other method is based on the spectroscopic measurements of the lifetimes $\tau_{\nu'}$. Since $A^{em}_{\nu'}$ varies little along the vibrational levels, $A^{pred}_{\nu'}$ can be obtained from $1/\tau_{\nu'} = A^{em}_{\nu'} + A^{pred}_{\nu'}$ by using A^{em}_2 as in Ref. [6].

Disagreement between recent experimental values [10] and early measurements [3,11] of the $A^{pred}_{\nu'}/A^{em}_{\nu'}$ ratio, presumably due to different thermal rotational distributions, calls for theoretical investigations of the effect of the temperature on the decay rates. Although predissociation rates including rotational motion have been calculated before [7], calculated photoemission rates reported in the literature [11] do not take into account the rotational motion, and therefore a detailed analysis of the effect of the temperature on the $A^{pred}_{\nu'}/A^{em}_{\nu'}$ ratio has not been carried out. Thus, in this work we present a theoretical investigation of the temperature effect on the two decay pathways, i.e., photoemission and predissociation, of the three isotopes $^{28}N_2^+$, $^{29}N_2^+$, and $^{30}N_2^+$. Our framework is based on the solution of the Schrödinger equation for the rovibronic motion of the molecular systems, followed by a Boltzmann statistical ensemble over the rotational states. For homonuclear systems the nuclear spins are considered in the wave functions, and therefore the ortho/para spin isomers are taken into account. Recent works on $B^2\Sigma_u^+/X^2\Sigma_g^+$ N_2^+ lasing [12,13] also motivate this investigation.

II. THEORY

The aim of this article is to calculate the photoemission rate $A^{em}_{\nu'}$ and the predissociation rate $A^{pred}_{\nu'}$ as a function of the temperature T for the three isotopes $^{28}N_2^+$, $^{29}N_2^+$, and $^{30}N_2^+$. Our theoretical framework is explained in three consecutive sets of calculations. The molecule is assumed to be aligned along the z axis. The first set of calculations concerns the electronic structure, i.e., the energies of the electronic states $X^2\Sigma_g^+$, $B\,^2\Sigma_u^+$, and $C\,^2\Sigma_u^+$, as well as the electronic dipole moment coupling $\langle X^2\Sigma_g^+|z|C\,^2\Sigma_u^+\rangle$ and the nonadiabatic coupling $\langle B\,^2\Sigma_u^+|d/dR|C\,^2\Sigma_u^+\rangle$, are calculated. These quantities are calculated in a discretized set of internuclear distances $\{R_i\}$ within the Born-Oppenheimer approximation. Second, the rovibrational wave functions $\Psi^{\alpha}_{\nu J}(\mathbf{R})$ for each potential energy curve, $\alpha = X, B, C$ (given by the electronic energy plus the nuclei-nuclei repulsion term), are calculated for the three isotopes $^{28}N_2^+$, $^{29}N_2^+$, and $^{30}N_2^+$. Note that each isotope has its own reduced nuclear mass. The rovibrational wave functions, electronic dipole, and nonadiabatic couplings allow us to calculate the photoemission rates $A^{em}_{\nu' J'}$ and

*jfperezt@uis.edu.co; http://ciencias.uis.edu.co/jfperezt/

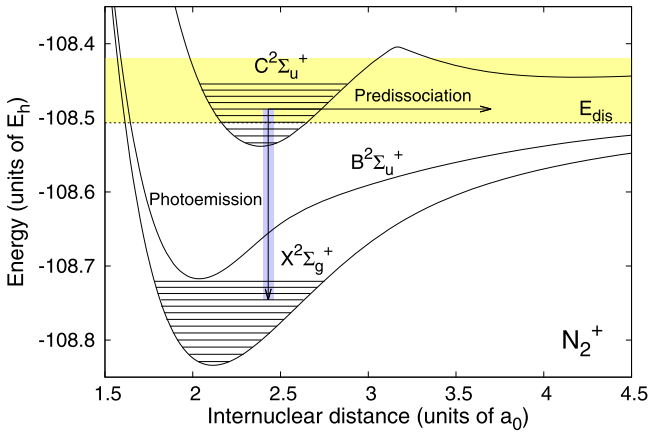

FIG. 1. Representation of the photoemission (vertical arrow) and the predissociation (horizontal arrow) pathways of N_2^+ ($C\,^2\Sigma_u^+, v', J'$). The vibrational states for $v' \geqslant 3$ of the $C\,^2\Sigma_u^+$ electronic state can either decay to the $X\,^2\Sigma_g^+$ electronic state, emitting one photon, or decay to the continuum of the $B\,^2\Sigma_u^+$ electronic state (yellow-shaded rectangle), breaking the molecular bond.

predissociative rates $A^{\text{pred}}_{v'J'}$ for reactions (1) and (2), respectively. Third, a Boltzmann distribution over the rotational states for a given temperature T is performed. For the $^{28}N_2^+$ and $^{30}N_2^+$ isotopes the nuclear spins are taken into account in order to describe the ortho and para spin isomers. Thus, the photoemission and predissociation rates as a function of the temperature for each vibrational state can be calculated by weighting the constant rates with the fractional population of each rotational state. Next we explain each set of calculations in more detail.

A. Electronic structure of N_2^+

We briefly recap the strategy developed in the previous work [8]. Accordingly, we assume that the rotational and vibrational motions do not interact with the electronic motion. Thus a fixed internuclear distance R is considered for the electronic calculations. In order to account for electronic correlation, first, a complete active-space self-consistent field [14] calculation with nine electrons in eight orbitals and an aug-cc-pV5Z [15] one-electron basis set (CASSCF(9,8)/aug-cc-pV5Z) is performed as implemented in MOLPRO [16]. To ensure smooth curves, the state average includes all doublet electronic states of the first three dissociation limits with equal weights. Due to limitation to the largest abelian subgroup D_{2h}, this includes the following irreducible representations: $7 \times A_g$, $6 \times B_{1g}$, $7 \times B_{1u}$, $6 \times A_u$, $7 \times B_{2u}$, $7 \times B_{3u}$, $7 \times B_{2g}$, and $7 \times B_{3g}$. As the second step a multireference configuration interaction including single and double excitations (MRCI-SD) [17,18] calculation as implemented in MOLPRO [16] follows. The Davidson correction is not employed. The electronic correlation of the ground and first excited state of N_2^+ has been analyzed in light of the quantum information theory and density-matrix renormalization-group method [19].

B. Rovibrational wave functions of N_2^+

We employ spherical coordinates to describe the nuclear motion, thus the stationary nuclear wave functions can be written as a product of a radial function times an angular function,

$$\Psi^{\alpha}_{vJ}(\mathbf{R}) = \frac{\psi^{\alpha}_{vJ}(R)}{R}\mathcal{Y}_{JM_J}(\Theta, \Phi), \tag{3}$$

where the angular functions $\mathcal{Y}_{JM_J}(\Theta, \Phi)$ correspond to the spherical harmonics. The $\psi^{\alpha}_{vJ}(R)$ part of the wave functions is then calculated by solving the radial Schrödinger equation,

$$\left[-\frac{\hbar^2 d^2}{2\mu dR^2} + \frac{J(J+1)}{2\mu R} + V^{\alpha}(R)\right]\psi^{\alpha}_{vJ}(R) = E^{\alpha}_{vJ}\psi^{\alpha}_{vJ}(R), \tag{4}$$

where α labels the $C\,^2\Sigma_u^+$, $B\,^2\Sigma_u^+$, and $X\,^2\Sigma_g^+$ electronic states and $\mu = M_A M_B/(M_A + M_B)$ the reduced nuclear mass. Concerning the $C\,^2\Sigma_u^+$ and $X\,^2\Sigma_g^+$ states, the Fourier grid Hamiltonian method [20] was employed for calculation of the bound rovibrational wave functions, whereas the continuum wave functions of $B^2\Sigma_u^+$ states were obtained by integrating the eigenvalue equation using the Numerov method at the rovibronic energies of the $C\,^2\Sigma_u^+$ state. The asymptotic amplitude of the continuum wave function was matched to

$$\psi^{\text{B}}_{E_{v'J'}}(R_{\max}) = \pi^{-1/2}\left(\frac{2\mu}{\hbar^2 E_{\text{kin}}}\right)^{1/4} \tag{5}$$

with

$$E_{\text{kin}} = E^{\text{C}}_{v'J'} - V^{\text{B}}(R_{\max}) - \frac{J'(J'+1)}{2\mu R_{\max}}, \tag{6}$$

where $R_{\max}$ is such that the stationary condition $|d\psi^{\text{B}}_{E_{v'J'}}(R)/dR|_{R=R_{\max}} = 0$ is satisfied, and it varies from $\sim 14.5a_0$ to $\sim 14.7a_0$ depending on the reduced mass μ of the isotope and on the J' value. The radiative rates were then calculated from the rovibrational energies and wave functions through the expressions [21]

$$k^{\text{R}}_{v'J'v''} = \frac{4}{3}\left(\frac{E^{\text{C}}_{v'J'} - E^{\text{X}}_{v''J'-1}}{\hbar c}\right)^3\left(\frac{e^2}{4\pi\varepsilon_0}\right)\left(\frac{J'}{2J'+1}\right) \times\left|\int \psi^{\text{C}}_{v'J'}(R)D_{\text{CX}}(R)\psi^{\text{X}}_{v''J'-1}(R)dR\right|^2, \tag{7}$$

$$k^{\text{P}}_{v'J'v''} = \frac{4}{3}\left(\frac{E^{\text{C}}_{v'J'} - E^{\text{X}}_{v''J'+1}}{\hbar c}\right)^3\left(\frac{e^2}{4\pi\varepsilon_0}\right)\left(\frac{J'+1}{2J'+1}\right) \times\left|\int \psi^{\text{C}}_{v'J'}(R)D_{\text{CX}}(R)\psi^{\text{X}}_{v''J'+1}(R)dR\right|^2, \tag{8}$$

where R and P stand for the R branch ($J'' = J' - 1$) and P branch ($J'' = J' + 1$), respectively, and $D_{\text{CX}}(R) = \langle X\,^2\Sigma_g^+|z|C\,^2\Sigma_u^+\rangle$ is the transition dipole function. The terms $(J'/2J'+1)$ and $(J'+1/2J'+1)$ entered, respectively, in Eqs. (7) and (8), correspond to the Hönl-London factors [22]. The photoemission rates summed over the final vibrational states, and therefore independent of the photon energy, were calculated as

$$A^{\text{em}}_{v'J'} = \sum_{v''}\left(k^{\text{P}}_{v'J'v''} + k^{\text{R}}_{v'J'v''}\right). \tag{9}$$

On the other hand, the predissociation rates were calculated through Fermi's golden rule,

$$A^{\rm pred}_{v'J'} = \frac{2\pi}{\hbar}\left|-\frac{\hbar^2}{2\mu}\int \psi^{\rm C}_{v'J'}(R)\hat{O}(R)\psi^{\rm B}_{E_{v'J'}}(R)dR\right|^2, \quad (10)$$

with

$$\hat{O}(R) = \left(2T^{(1)}_{\rm CB}(R)\frac{d}{dR} + T^{(2)}_{\rm CB}(R)\right). \quad (11)$$

The coupling function $T^{(1)}_{\rm CB}(R)$, defined by

$$T^{(1)}_{\rm CB}(R) = \int \Phi_{\rm B}(\mathbf{x};R)\frac{d}{dR}\Phi_{\rm C}(\mathbf{x};R)d\mathbf{x}, \quad (12)$$

was calculated using finite differences as implemented in MOLPRO [16], whereas the coupling function $T^2_{\rm CB}(R)$ was estimated to be (see Ref. [8])

$$T^{(2)}_{\rm CB}(R) \approx \frac{d}{dR}T^{(1)}_{\rm CB}(R). \quad (13)$$

C. Rotational statistical ensemble of N_2^+

In order to distinguish between the different isotopes of N_2^+ beyond the reduced mass μ entered in Eq. (4) and to incorporate the temperature to our observables, we resort to a statistical ensemble over the rotational states. For simplicity we start by discussing the $^{29}N_2^+$ isotope. The fraction of molecules in the rotational state J' at temperature T is given by

$$\chi_{v'J'}(T) = \frac{(2J'+1)\exp\left[-\left(E^{\rm C}_{v'J'} - E^{\rm C}_{v'0}\right)/k_BT\right]}{Q_{v'}(T)}, \quad (14)$$

with $Q_{v'}(T)$ the corresponding partition function

$$Q_{v'}(T) = \sum_{J'}(2J'+1)\exp\left[-\left(E^{\rm C}_{v'J'} - E^{\rm C}_{v'0}\right)/k_BT\right]. \quad (15)$$

Note that $\sum_{J'}\chi_{v'J'} = 1$ for each vibrational state v'. Then the photoemission and predissociation rates at temperature T were calculated as

$$A^{\rm em}_{v'}(T) = \sum_{J'}\chi_{v'J'}(T)A^{\rm em}_{v'J'}, \quad (16)$$

$$A^{\rm pred}_{v'}(T) = \sum_{J'}\chi_{v'J'}(T)A^{\rm pred}_{v'J'}. \quad (17)$$

The photoemission spectrum $I(\lambda)$ vs λ at temperature T was built up as

$$I(\lambda) = \chi_{v'J'}(T)\frac{k^{\rm P}_{v'J'v''}(\lambda) + k^{\rm R}_{v'J'v''}(\lambda)}{A^{\rm em}_{v'J'} + A^{\rm pred}_{v'J'}}, \quad (18)$$

$$\lambda = \frac{hc}{E^{\rm C}_{v'J'} - E^{\rm X}_{v''J''}}, \quad (19)$$

with $I(\lambda)$ the relative photoemission intensity and λ the wavelength of the emitted photon.

For the isotopes $^{28}N_2^+$ and $^{30}N_2^+$ the statistical ensemble is a little different from that for $^{29}N_2^+$. Due to the indistinguishability of the nuclei, the sample must be considered a mixture of the ortho and para modifications, i.e., spin isomers of the nitrogen [4]. $^{28}N_2^+$ is formed by bosons (two nuclei of ^{14}N with integer nuclear spin $I = 1$), whereas $^{30}N_2^+$ is formed by fermions (two nuclei of ^{15}N with half-integer nuclear spin $I = 1/2$). Since radiative and predissociative relaxation occur without spin conversion, each sample of $^{28}N_2^+$ and $^{30}N_2^+$ must be considered a mixture of two molecular spin isomers, i.e., ortho and para molecular nitrogen. Each kind of isomer has its own partition function. The two partition functions are given by

$$Q^{\rm ortho}_{v'}(T) = (I+1)(2I+1)\sum_{J'}(2J'+1) \times \exp\left[-\left(E^{\rm C}_{v'J'} - E^{\rm C}_{v'J'_{\rm min}}\right)/k_BT\right], \quad (20)$$

$$Q^{\rm para}_{v'}(T) = I(2I+1)\sum_{J'}(2J'+1) \times \exp\left[-\left(E^{\rm C}_{v'J'} - E^{\rm C}_{v'J'_{\rm min}}\right)/k_BT\right], \quad (21)$$

with the fraction of molecules in rotational state J' for each isomer given by the statistical weights

$$\chi^{\rm ortho}_{v'J'}(T) = (I+1)(2I+1)\left(2J'+1\right) \times \frac{\exp\left[-\left(E^{\rm C}_{v'J'} - E^{\rm C}_{v'J'_{\rm min}}\right)/k_BT\right]}{Q^{\rm ortho}_{v'}(T) + Q^{\rm para}_{v'}(T)}, \quad (22)$$

$$\chi^{\rm para}_{v'J'}(T) = I(2I+1)(2J'+1) \times \frac{\exp\left[-\left(E^{\rm C}_{v'J'} - E^{\rm C}_{v'J'_{\rm min}}\right)/k_BT\right]}{Q^{\rm ortho}_{v'}(T) + Q^{\rm para}_{v'}(T)}, \quad (23)$$

where $J'_{\rm min}$ is 0 or 1 depending on the parity restriction of the rotational wave function. Note that $\sum_{J'}(\chi^{\rm ortho}_{v'J'} + \chi^{\rm para}_{v'J'}) = 1$. Since the total wave function of $^{28}N_2^+$ (a boson) must be symmetric, and the wave function of the electronic state $C\,^2\Sigma_u^+$ is antisymmetric with respect to the nuclei interchange, the ortho (symmetric) nuclear spin states are restricted to having antisymmetric rotational wave functions, therefore the summation in Eq. (20) and J' appearing in Eq. (22) are restricted to odd values. Accordingly, the para (antisymmetric) nuclear spin states of the $C\,^2\Sigma_u^+$ electronic state are restricted to symmetric rotational wave functions with even values of J'. For the isotope $^{30}N_2^+$ (a fermion) the total wave function must be antisymmetric, therefore for the electronic state $C\,^2\Sigma_u^+$, the ortho spin states are restricted to even values of J', whereas the para spin states are restricted to odd values of J'. So the photoemission and predissociation rates at temperature T result from the weighted rates of the mixture of the spin isomers,

$$A^{\rm em}_{v'}(T) = \sum_{J'}\chi^{\rm ortho}_{v'J'}(T)A^{\rm em}_{v'J'} + \sum_{J'}\chi^{\rm para}_{v'J'}(T)A^{\rm em}_{v'J'}, \quad (24)$$

$$A^{\rm pred}_{v'}(T) = \sum_{J'}\chi^{\rm ortho}_{v'J'}(T)A^{\rm pred}_{v'J'} + \sum_{J'}\chi^{\rm para}_{v'J'}(T)A^{\rm pred}_{v'J'}, \quad (25)$$

and the photoemission spectrum is built up as a superposition of the two spectra $I^{\rm ortho}(\lambda)$ and $I^{\rm para}(\lambda)$. Note that observables considered here can be obtained from rovibrational energies, Eq. (4), photoemission rates, Eqs. (7) and (8), and predissociation rates, Eq. (10); this information is given as Supplemental Material [23].

TABLE I. Comparison of calculated and measured relative vibrational energies $\Delta E^{C}_{\nu'0} = (E^{C}_{\nu'0} - E^{C}_{00})$ (meV), photoemission rates $A^{em}_{\nu'0}/10^7$ s^{-1}, and predissociation rates $A^{pred}_{\nu'10}/10^7$ s^{-1} of the $C\,^2\Sigma_u{}^+$ electronic state of $^{28}N_2{}^+$. Results of the present work correspond to para-$^{28}N_2{}^+$.

Quantity	Source	ν': $^{28}N_2{}^+$								
		0	1	2	3	4	5	6	7	8
$\Delta E^{C}_{\nu'0}$	This work	0	254	505	753	998	1239	1476	1709	1937
$\Delta E^{C}_{\nu'0}$	Ref. [24] theor.	0	254	504	751	994	1233	1468	1699	1924
$\Delta E^{C}_{\nu'}$	Ref. [25] expt.	0	248	500	748	993	1234	1471	1703	1931
$A^{em}_{\nu'0}$	This work	1.31	1.37	1.42	1.46	1.49	1.51	1.52	1.53	1.53
$A^{em}_{\nu'0}$	Ref. [11] theor.	1.56	1.61	1.69	1.71	1.73	1.73			
$A^{em}_{\nu'}$	Ref. [6] expt.		1.29	1.12(5)						
$A^{pred}_{\nu'10}$	This work	0	0	0	14.7	31.3	59.6	102.5	160.6	239.7
$A^{pred}_{\nu'10}$	Ref. [7] theor.	0	0	0	6.4	14.6	18.6	50	82	124
$A^{pred}_{\nu'}$	Ref. [7] expt.	0	0	0	13(2)	24(6)	50(10)	82(23)	100(38)	278
$A^{pred}_{\nu'}$	Ref. [6] expt.	0	0	0	24(6)	19(4)	19(4)			

III. RESULTS

Because of its natural abundance, $^{28}N_2{}^+$ is the isotope most studied experimentally. Therefore, as a test, we first compare our results with the relevant physical quantities available in the literature concerning the 2N system. Table I gathers the experimental and theoretical data for the vibrational energy spacing of the $C\,^2\Sigma_u{}^+$ electronic state and the photoemission and predissociation rates. To be consistent with the reported theoretical works, we present values of photoemission rates for $J' = 0$ and predissociation rates for $J' = 10$ (see Roche *et al.* [7]). In general our results are in good agreement with pioneer works by Erman [6], Roche *et al.* [7], Baltzer *et al.* [25], and Ehresmann *et al.* [24]. In particular, our photoemission rates for $\nu' = 1$ and $\nu' = 2$ are in better agreement with the experimental values reported by Erman [6], which yield lifetimes of 72.3 and 70.4 ns, respectively. On the other hand, our predissociation rates are closer to experimental values reported by Roche *et al.* [7]. It is remarkable that the photoemission and predissociation rates increase as the vibrational quantum number ν' increases. Nevertheless, changes in the photoemission rates occur in the range between 1.31×10^7 and 1.53×10^7 s^{-1}, while the predissociation rates change greatly, from 14.7×10^7 to 239.7×10^7 s^{-1}, upon going from $\nu' = 3$ to $\nu' = 8$. Because $A^{pred}_{\nu'} \gg A^{em}_{\nu'}$ for any J', the lifetime for vibrational states with $\nu' \geqslant 3$ is governed by the predissociation process, yielding 6.8 ns for $\nu' = 3$ and 0.42 ns for $\nu' = 8$. Thus, relaxation of the $C\,^2\Sigma_u{}^+$ state is about 10 times faster for vibrational states $\nu' \geqslant 3$ compared to vibrational states $\nu' = 0$, 1, and 2. Note that the natural energy width $\Delta = \hbar/\tau$ for vibrational states $\nu' = 3$ and $\nu' = 8$, 9.7×10^{-5}, and 1.6×10^{-3} meV, respectively, are too small compared to the spacing of the energy levels (753–505) meV = 248 meV and (1937–1709) meV = 228 meV (see Table I), and therefore effects of overlapping resonances [26] and perturbation of vibrational levels ν' through the dissociation continuum [27] can be neglected.

Table II lists our calculated photoemission ($J' = 0$) and predissociation ($J' = 10$) rates for isotopes $^{29}N_2{}^+$ and $^{30}N_2{}^+$. The predissociation rates are compared with the theoretical and experimental values reported by Roche *et al.* [7]. For isotope $^{29}N_2{}^+$ the predissociation is still the dominant relaxation process, whereas for isotope $^{30}N_2{}^+$ photoemission dominates for vibrational states $\nu' = 3$, 4, and 5, while predissoci-

TABLE II. Calculated photoemission rates $A^{em}_{\nu'0}/10^7$ s^{-1} and predissociation rates $A^{pred}_{\nu'10}/10^7$ s^{-1} of the $C\,^2\Sigma_u{}^+$ electronic state of $^{29}N_2{}^+$ and ortho-$^{30}N_2{}^+$. A comparison is done with calculated and measured predissociation rates reported by Roche *et al.* [7].

Quantity	Source	ν'					
		3	4	5	6	7	8
			$^{29}N_2{}^+$				
$A^{em}_{\nu'0}$	This work	1.46	1.49	1.51	1.52	1.53	1.53
$A^{pred}_{\nu'10}$	This work	3.79	7.65	15.11	25.65	39.84	58.37
$A^{pred}_{\nu'10}$	Ref. [7] theor.	0.97	2.32	4.7	8.5	14.	21.2
$A^{pred}_{\nu'}$	Ref. [7] expt.	2.33 ± 0.35	4.60 ± 0.60	8.9 ± 1.1	17.4 ± 3.2	23.3 ± 5	66 ± 35
			$^{30}N_2{}^+$				
$A^{em}_{\nu'0}$	This work	1.45	1.48	1.51	1.52	1.53	1.53
$A^{pred}_{\nu'10}$	This work	0.32	0.81	1.41	2.74	4.63	7.64
$A^{pred}_{\nu'10}$	Ref. [7] theor.	0.50	1.08	2.08	3.7	6.0	9.3
$A^{pred}_{\nu'}$	Ref. [7] expt.	1.26 ± 0.13	2.22 ± 0.2	4.8 ± 0.4	22.3 ± 5	22.0 ± 4	58 ± 25

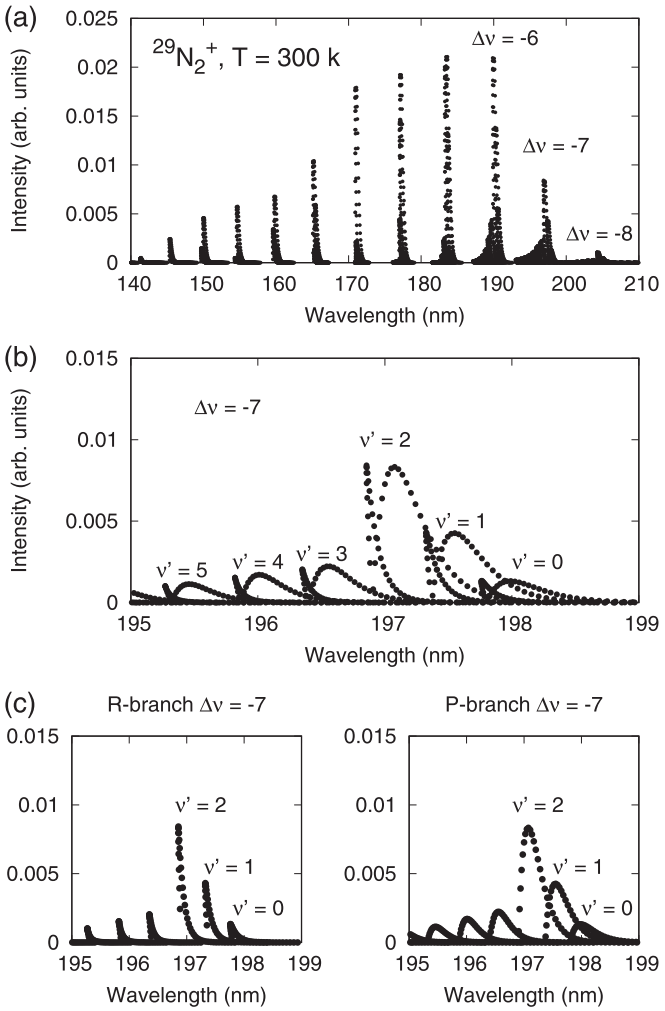

FIG. 2. Photoemission spectrum of $^{29}N_2^+(C\,^2\Sigma_u^+)$ at $T = 300$ K; the wavelength is given by $\lambda = hc/(E^{C}_{\nu' J'} - E^{X}_{\nu'' J''})$. (a) Spectrum for wavelengths ranging from 140 to 210 nm (i.e., $\Delta\nu$ from +3 to −8; $\Delta\nu = \nu' - \nu''$). (b) Window displaying the photoemission signal for the group $\Delta\nu = -7$; subgroups corresponding to the initial states $\nu' = 0$, 1, 2, 3, 4, and 5 are indicated. (c) R branches and P branches of the photoemission signals of the group $\Delta\nu = -7$.

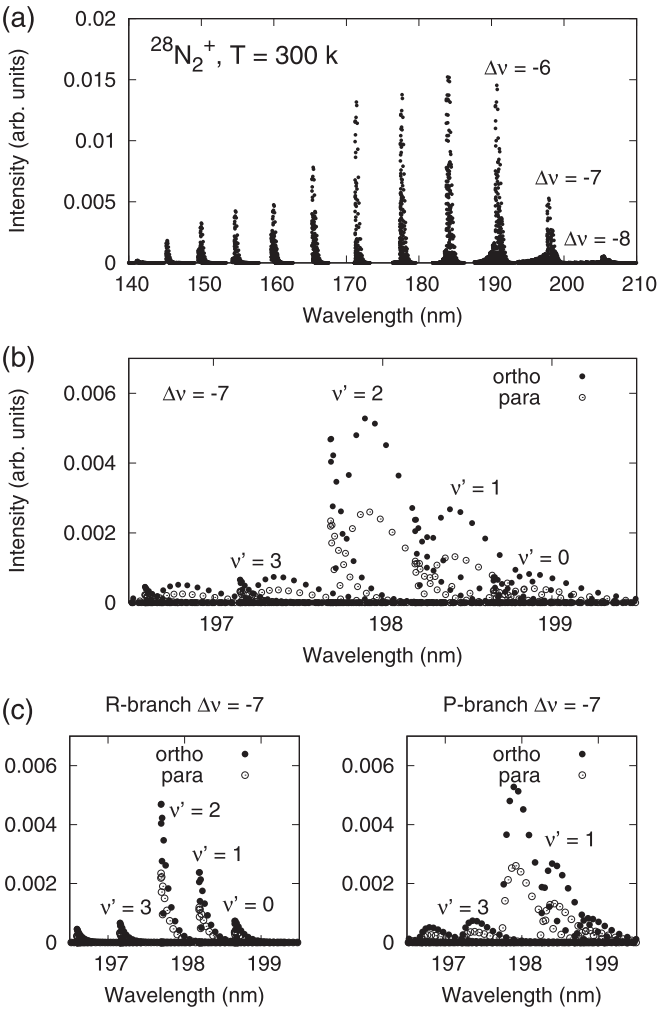

FIG. 3. Photoemission spectrum of $^{28}N_2^+(C\,^2\Sigma_u^+)$ at $T = 300$ K; the wavelength is given by $\lambda = hc/(E^{C}_{\nu' J'} - E^{X}_{\nu'' J''})$. (a) Spectrum with wavelengths ranging from 140 to 210 nm (i.e., $\Delta\nu$ from +3 to −8; $\Delta\nu = \nu' - \nu''$). (b) Window displaying the photoemission signal for the group $\Delta\nu = -7$; subgroups corresponding to the initial states $\nu' = 0$, 1, 2, and 3 are indicated. (c) R branches and P branches of the photoemission signals of the group $\Delta\nu = -7$. Filled and open circles correspond to the ortho and para spin isomers, respectively.

ation dominates from $\nu \geqslant 6$. It should be noted that the agreement with experimental data is better for $^{29}N_2^+$ than for $^{30}N_2^+$, presumably due to the fact that the photoemission and predissociation rates are similar and too small compared to those for $^{28}N_2^+$. So far, our results for the isotopes $^{28}N_2^+$ and $^{29}N_2^+$ are in good agreement with the reported experimental values, while for the isotope $^{30}N_2^+$ the agreement is acceptable.

Next we describe the photoemission spectrum for the three isotopes; they can be compared with experimental spectra reported by Holland *et al.* [28], van de Runstraat *et al.* [1], and Govers *et al.* [3]. Figure 2 shows $I(\lambda)$ at 300 K for the $^{29}N_2^+$ system. Figure 2(a) displays the relative photoemission intensity (arbitrary units) calculated from $\lambda = 140$ nm to $\lambda = 210$ nm. Twelve groups of signals can be appreciated. Each group is made up of all the transitions between two vibrational states with the same $\Delta\nu$. For example, the group around 197 nm corresponds to the vibrational transitions $\nu' \to \nu' + 7$. Each group is therefore formed by the photoemission from different initial vibrational states ν', i.e., a band. Figure 2(b) displays the different bands ν' of the group $\Delta\nu = -7$. Each band is composed of two branches, the R branch (the $J' \to J' - 1$ transition) and the P branch (the $J' \to J' + 1$ transition). Figure 2(c) displays the two branches of the bands $\nu' = 0$, 1, 2, 3, 4, and 5 of the group $\Delta\nu = -7$. Thus, each point in the spectrum represents a single transition, $\nu' J' \to \nu'' J''$. Note that the peak intensities of bands displayed in Figs. 2(b) and 2(c) increase for $\nu' = 0$, 1, and 2 and then decrease abruptly to more or less a constant value for $\nu' = 3$, 4, and 5. This behavior is a signature of the dominant predissociation process of vibrational levels $\nu' \geqslant 3$. From the P branch of band $\nu' = 2$ [see Fig. 2(c), right panel] one can recognize that the peak intensity occurs at $J' = 7$, which corresponds to the most populated rotational state of $^{29}N_2^+$ at 300 K.

Figures 3 and 4 show the photoemission spectrum for $^{28}N_2^+$ at 300 and 50 K, respectively. The effect of the temper-

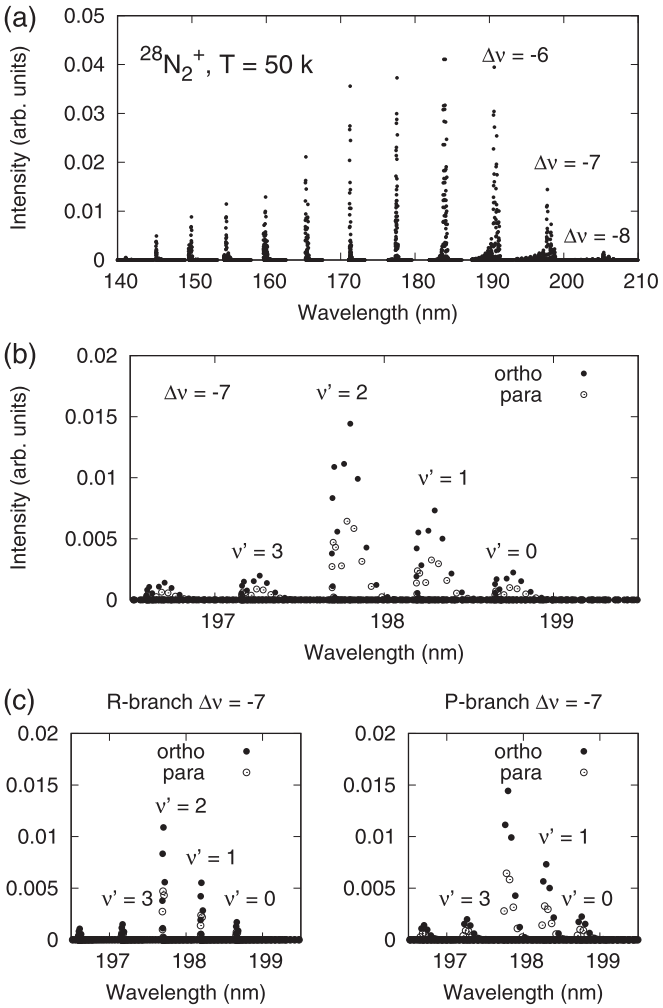

FIG. 4. Photoemission spectrum of $^{28}N_2^+(C\,^2\Sigma_u^+)$ at $T = 50$ K. For details see the caption to Fig. 3.

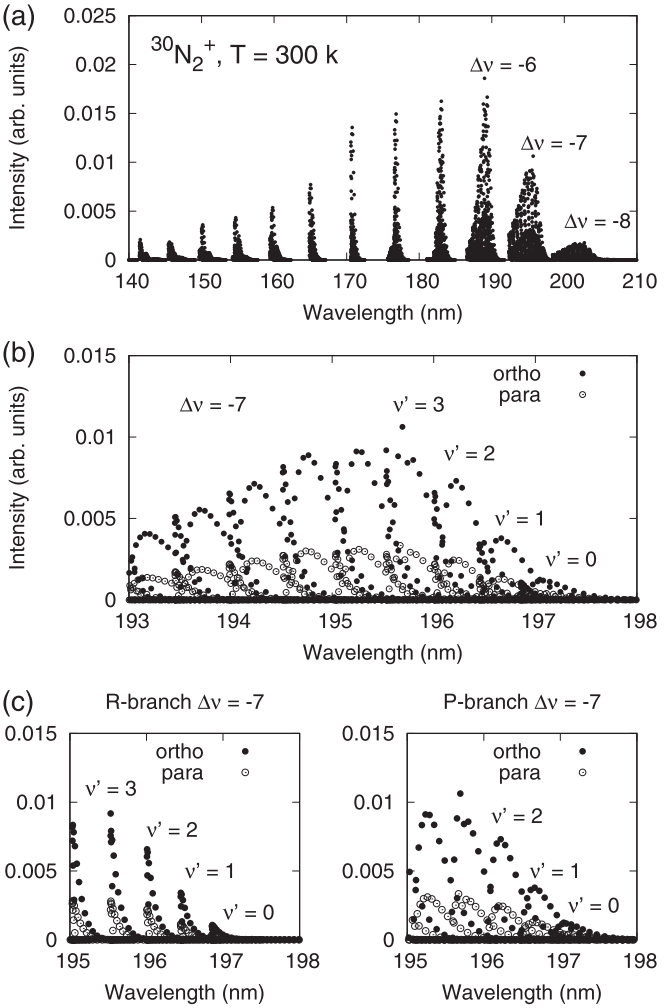

FIG. 5. Photoemission spectrum of $^{30}N_2^+(C\,^2\Sigma_u^+)$ at $T = 300$ K; the wavelength is given by $\lambda = hc/(E^{C}_{\nu'J'} - E^{X}_{\nu''J''})$. (a) Spectrum with wavelengths ranging from 140 to 210 nm (i.e., $\Delta\nu$ from +2 to −8; $\Delta\nu = \nu' - \nu''$). (b) Window displaying the photoemission signal for the group $\Delta\nu = -7$; subgroups corresponding to the initial states $\nu' = 0$, 1, 2, and 3 are indicated. (c) R branches and P branches of the photoemission signals of the group $\Delta\nu = -7$. Filled and open circles correspond to the ortho and para spin isomers, respectively.

ature on the photoemission spectrum can be plainly seen. The same trends found for isotope $^{29}N_2^+$ (shown in Fig. 2) hold for isotope $^{28}N_2^+$ at both temperatures. The spectra displayed correspond to the mixture $I^{\text{ortho}}(\lambda)$ and $I^{\text{para}}(\lambda)$. Figures 3(b) and 4(b) show the $\nu' = 0$, 1, 2, 3, and 4 bands of the group $\Delta\nu = -7$. Filled circles represent ortho-$^{28}N_2^+$, whereas open circles show para-$^{28}N_2^+$. Note that the intensities of ortho-$^{28}N_2^+$ are about a factor of 2 larger than those of para-$^{28}N_2^+$ and they alternate. This intensity alternation in the ratio 2:1, also observed in the Raman spectrum of N_2 [29], is a consequence of the relative abundance of the spin isomers given by $R = (I + 1)/I$ with $I = 1$ for $^{28}N_2^+$. Figures 3(c) and 4(c) exhibit the corresponding R and P branches. Similarly to $^{29}N_2^+$, $^{28}N_2^+$ also reveals an abrupt decay of the photoemission signal for $\nu' \geqslant 3$ due to the dominant predissociation. As expected, the bands are sharper at 50 K [compare Fig. 3(b) and Fig. 4(b)]. At 50 K the most populated rotational states are $J' = 3$ and $J' = 2$ for the ortho and para spin isomers, respectively.

The photoemission spectrum of $^{30}N_2^+$ at 300 K is shown in Fig. 5. As in the case of the $^{28}N_2^+$ system, the spectrum of $^{30}N_2^+$ is also made up of a mixture, i.e., $I^{\text{ortho}}(\lambda)$ and $I^{\text{para}}(\lambda)$. Note that the peak intensities of the ortho isomer are about a factor of 3 of the peak intensities of the para isomer, according to the $R = (I + 1)/I$ ratio for $I = 1/2$. Such an alternation of 3:1 in the intensity of the signals has also been observed in spectroscopic measurements of $^{30}N_2^+$ and used to determine the nuclear spin of the ^{15}N isotope [30,31]. We would like to remark that in this case no abrupt decay is observed in the photoemission spectrum as in the previous systems. This is due to the comparable magnitudes of $A^{\text{em}}_{\nu'}$ and $A^{\text{pred}}_{\nu'}$ (see results for $^{30}N_2^+$ in Table II) and therefore the lack of a dominant process.

Recently, Hrodmarsson *et al.* [10] have reported new predissociation/photoemission ratios for the isotopes $^{28}N_2^+$ and $^{30}N_2^+$. Their results are based on the ratio $I(N^+)/I(N_2^+)$ of the signals measured in a mass spectrometer after photoionization of N_2 with synchrotron radiation. Table III gathers our results calculated with Eqs. (24) and (25) at two temperatures. Experimental results reported by

TABLE III. Calculated predissociation/photoemission ratios $A^{\rm pred}_{v'}/A^{\rm em}_{v'}$ at $T = 50$ K and $T = 300$ K. Experimental values of predissociation/photoemission ratios reported by Govers *et al.* (1975) [3], Ehresmann *et al.* (2006) [11], and Hrodmarsson *et al.* (2019) [10] are also included.

	v'					
Source	3	4	5	6	7	8
			$^{28}N_2^+$			
This work (50 K)	10.2	20.7	38.9	66.2	103.3	154.2
This work (300 K)	10.1	21.0	39.5	67.3	105.0	156.9
Ref. [11] expt.	10.0	18	27	61		
Ref. [3] expt.	9.8(8.5–11.5)	18(15–22)	33(29–40)	52(42–70)	60(45–90)	160(95–480)
Ref. [10] expt.	32(25–44)	55(36–110)	$\geqslant$332	$\geqslant$332		
			$^{29}N_2^+$			
This work (50 K)	2.50	4.59	9.00	15.13	23.41	34.31
This work (300 K)	2.75	5.38	10.47	17.65	27.28	40.05
Ref. [3] expt.	1.79 ± 0.20	3.66 ± 0.45	6.1 ± 0.6	10.9 ± 1.5	14(11–16)	38(8–48)
			$^{30}N_2^+$			
This work (50 K)	0.04	0.74	1.27	2.41	4.00	6.49
This work (300 K)	0.13	0.51	0.87	1.67	2.80	4.60
Ref. [3] expt.	0.98 ± 0.10	1.53 ± 0.10	3.19 ± 0.20	17.6 ± 3.5	13.2 ± 2.5	33(13–41)
Ref. [10] expt.	1.70 ± 0.24	3.17 ± 0.18	7.3(6.9-7.8)	46(42-52)	19(18-21)	$\geqslant$24

Hrodmarsson *et al.* (2019) [10], Ehresmann *et al.* (2006) [11], and Govers *et al.* (1975) [3] are also included. The temperature for experiments on $^{28}N_2^+$ and $^{30}N_2^+$ carried out by Hrodmarsson *et al.* is estimated to be 50 K with $J = 3$ as the maximum of the rotational distribution [10], whereas the temperature for experiments reported by Govers *et al.* is estimated to be 300 K with $J = 9$ as the maximum of the rotational distribution [3]. For this reason we report our results for 50 and 300 K. Note the differences in the experimental results reported by Hrodmarsson *et al.* and those reported by Govers *et al.* and Ehresmann *et al*. It was suggested that differences in the predissociation/photoemission ratios be attributed to the thermal rotational distributions in each experiment [10]. Figure 6 exhibits the predissociation/photoemission ratio as a function of the temperature for the three isotopes $^{28}N_2^+$, $^{29}N_2^+$, and $^{30}N_2^+$. As can be seen, the effect of the temperature is more pronounced for $^{30}N_2^+$, barely visible for $^{29}N_2^+$, and negligible in $^{28}N_2^+$. These trends agree with theoretical results reported by Roche *et al.* [7], who studied the predissociation/photoemission ratio as a function of the rotational quantum number J'. In particular, we found that for $^{30}N_2^+$ the photoemission prevails for $v' = 3$ and $v' = 4$, whereas for $v' = 5$ predissociation prevails at least until ca. 300 K, where photoemission becomes more important. For vibrational states $v \geqslant 6$ predissociation dominates at least until 400 K. In order to guarantee reliability of the results, a maximum rotational quantum number of $J'_{\rm max} = 40$ was included in the calculations, yielding a population of $\chi^{\rm ortho}_{v'J'=40} = 0.0002$ and $\chi^{\rm para}_{v'J'=39} = 0.0001$ at 400 K for all vibrational levels v', with $J' = 10$ ($\chi^{\rm ortho}_{v'J'=10} = 0.0909$) and $J' = 9$ ($\chi^{\rm para}_{v'J'=9} = 0.0307$) the most populated rotational states.

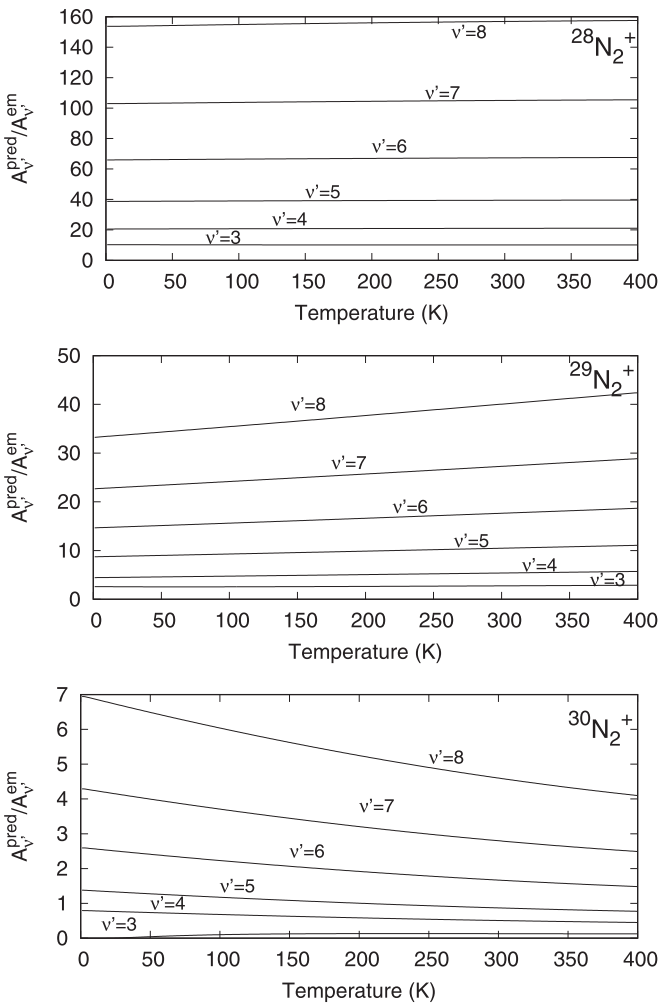

FIG. 6. Predissociation/photoemission ratios for different vibrational states v' as a function of the temperature.

IV. SUMMARY AND CONCLUSIONS

We have studied the effect of the temperature on the predissociation and photoemission rates of the molecular

isotopes $^{28}N_2^+$, $^{29}N_2^+$, and $^{30}N_2^+$ in the $C\,^2\Sigma_u^+$ electronic state. For homonuclear systems, the ortho and para spin isomers have been considered, giving rise to a detailed description of the photoemission spectrum, e.g., alternating intensities of successive rotational lines due to the statistical weights of the spin isomers are visible. For the $^{28}N_2^+$ and $^{29}N_2^+$ isotopes the predissociation can be deduced from the photoemission spectrum as a strong decay of the signal for $\nu' \geqslant 3$, whereas for the $^{30}N_2^+$ isotope predissociation can barely be appreciated from the photoemission spectrum. From our calculations we can conclude that predissociation is the dominant decay process for isotopes $^{28}N_2^+$ and $^{29}N_2^+$. We have also studied the effect of the temperature on the predissociation/photoemission ratio for several vibrational levels ν'. Our results suggest that differences in the predissociation/photoemission ratio reported by Hrodmarsson *et al.* versus those reported by Govers *et al.* [3] and Ehresmann *et al.* [11] cannot be attributed to the thermal distribution of the rotational states. However, we should state that our theoretical framework considers only direct predissociation of the $C\,^2\Sigma_u^+$ state and that accidental predissociation [32,33], not included in our calculations, might play an important role at low rotational temperatures. A theoretical description of this phenomenon with both direct and accidental predissociation pathways is being pursued.

ACKNOWLEDGMENTS

C. Forero, J. Villabona, and J. F. Pérez-Torres are grateful for the generous allocation of computer time from the SC3 Supercomputing Center of the Universidad Industrial de Santander (UIS). We benefited from the support of Project 2411 of Vicerrectoría de Investigación y Extensión UIS.

[1] C. A. van de Runstraat, F. J. de Heer, and T. R. Govers, Excitation and decay of the $C^2\Sigma_u^+$ state of N_2^+ in the case of electron impact on n_2, Chem. Phys. **3**, 431 (1973).

[2] T. R. Govers, F. C. Fehsenfeld, D. L. Albritton, P. G. Fournier, and J. Fournier, Molecular isotope effects in the thermal-energy charge exchange between He^+ and N_2, Chem. Phys. Lett. **26**, 134 (1974).

[3] T. R. Govers, C. A. van de Runstraat, and F. J. de Heer, Excitation and decay of the $C^2\Sigma_u^+$ state of N_2^+ following collisions of the ions with N_2 isotopes, Chem. Phys. **9**, 285 (1975).

[4] G. Herzberg, *Molecular Spectra and Molecular Structure. I. Spectra of Diatomic Molecules*, 2nd ed., Vol. 8 (D. Van Nostrand, New Hyde Park, NY, 1963).

[5] A. Lofthus and P. H. Krupenie, The spectrum of molecular nitrogen, J. Phys. Chem. Ref. Data **6**, 113 (1977).

[6] P. Erman, Direct measurement of the N_2^+C state predissociation probability, Phys. Scripta **14**, 51 (1976).

[7] A. L. Roche and J. Tellinghuisen, Predissociation and perturbations in the $C^2\Sigma_u^+$ state of N_2^+ from interaction with the $B^2\Sigma_u^+$ state, Mol. Phys. **38**, 129 (1979).

[8] B. Paulus, J. F. Pérez-Torres, and C. Stemmle, Time-dependent description of the predissociation of N_2^+ in the $C^2\Sigma_u^+$ state, Phys. Rev. A **94**, 053423 (2016).

[9] R. de L Kronig, Über den spontanen Zerfall zweiatomiger Moleküle, Z. Phys. **50**, 347 (1928).

[10] H. R. Hrodmarsson, R. Thissen, D. Dowek, G. A. García, L. Nahon, and T. R. Govers, Isotope effects in the predissociation of excited states of N_2^+ produced by photoionization of $^{14}N_2^+$ and $^{15}N_2^+$ at energies between 24.2 and 25.6 eV, Front. Chem. **7**, 222 (2019).

[11] A. Ehresmann, L. Werner, S. Klumpp, P. V. Demekhin, M. P. Lemeshko, V. L. Sukhorukov, K.-H. Schartner, and H. Schmoranzer, Predissociation of the $N_2^+(C^2\Sigma_u^+)$ state observed via $C^2\Sigma_u^+ \rightarrow X^2\Sigma_g^+$ fluorescence after resonant $1s^{-1}\pi^*$ excitation of N_2 molecule, J. Phys. B: At. Mol. Opt. Phys. **39**, L119 (2006).

[12] M. Lytova, M. Richter, F. Morales, O. Smirnova, M. Ivanov, and M. Spanner, N_2^+ lasing: Gain and absorption in the presence of rotational coherence, Phys. Rev. A **102**, 013111 (2020).

[13] H. Li, E. Lötstedt, H. Li, Y. Zhou, N. Dong, L. Deng, P. Lu, T. Ando, A. Iwasaki, Y. Fu, S. Wang, J. Wu, K. Yamanouchi, and H. Xu, Giant Enhancement of Air Lasing by Complete Population Inversion in N_2^+, Phys. Rev. Lett. **125**, 053201 (2020).

[14] P. J. Knowles and H.-J. Werner, An efficient second-order MC SCF method for long configuration expansions, Chem. Phys. Lett. **115**, 259 (1985).

[15] R. A. Kendall, T. H. Dunning, and R. J. Harrison, Electron affinities of the first-row atoms revisited. Systematic basis sets and wave functions, J. Chem. Phys. **96**, 6796 (1992).

[16] H.-J. Werner, P. J. Knowles, G. Knizia, F. R. Mamby, M. Schütz, Molpro: a generalpurpose quantum chemistry program package, WIREs Comput. Mol. Sci. **2**, 242 (2012); H.-J. Werner, P. J. Knowles, G. Knizia, F. R. Manby, M. Schütz *et al.*, MOLPRO,version 2019.2, a package of ab initio programs, see https://www.molpro.net.

[17] H.-J. Werner and P. J. Knowles, An efficient internally contracted multiconfiguration-reference configuration method, J. Chem. Phys. **89**, 5803 (1988).

[18] P. J. Knowles and H.-J. Werner, An efficient method for the evaluation of coupling coefficients in configuration interaction calculation, Chem. Phys. Lett. **145**, 514 (1988).

[19] C. Stemmle, B. Paulus, and Ö. Legeza, Analysis of electron-correlation effects in strongly correlated systems (N_2 and N_2^+) by applying the desnity-matrix renormalization-group method and quantum information theory, Phys. Rev. A **97**, 022505 (2018).

[20] C. C. Marston and G. G. Balint-Kurti, The Fourier grid Hamiltonian method for bound states eigenvalues and eigenfunctions, J. Chem. Phys. **91**, 3571 (1989).

[21] B. H. Bransden and C. J. Joachain, *Physics of Atoms and Molecules* (Longman, London, 1983).

[22] H. Hönl and F. London, Über die Instensitäten der Bandenlinien, Z. Phys. **33**, 803 (1925).

[23] See Supplemental Material at http://link.aps.org/supplemental/10.1103/PhysRevA.102.032802 for information on how observables considered here were obtained.

[24] A. Ehresmann, L. Werner, S. klumpp, S. Lucht, H. Schmoranzer, S. Mickat, R. Schill, K.-H. Schartner, P.

Demekhin, M. P. Lemeshko, and V. L. Sukhorukov, Studying the $N_2^+(C\,^2\Sigma_u^+ \rightarrow \chi\,^2\Sigma_g^+)$ fluorescence excited via the $1s^{-1}\pi^*$ resonance, J. Phys. B: At. Mol. Opt. Phys. **39**, 283 (2006).

[25] P. Baltzer, M. Larsson, L. Karlsson, B. Wannberg, and M. Carlsson Göthe, Inner-valence states of N_2^+ studied by uv photoelectron spectroscopy and configuration-interaction calculations, Phys. Rev. A **46**, 5545 (1992).

[26] H. Feshbach, The unified theory of nuclear reactions. III. Overlapping resonances*, Ann. Phys. **43**, 410 (1967).

[27] A. Ehresmann, L. Werner, S. Klumpp, H. Schmoranzer, P. V. Demekhin, B. M. L. V. L. Sukhorukov, S. Mickat, S. Kammer, B. Zimmermann, and K.-H. Schartner, De-excitation dynamics of Rydberg states in O_2: II. Vibrational and rotational structure of $2\sigma_u^{-1}(c^4\Sigma_u^-)(ns\ nd)\sigma_g^3\Sigma_u^-(v=0,1)$ states, J. Phys. B: At. Mol. Opt. Phys. **37**, 4405 (2004).

[28] R. F. Holland and W. B. Maier II, Production of light by collisions of 2.5–490 eV He^+ with N_2: NI, N_2^+ second negative, and unresolved emissions between 1200 and 3200 Å, J. Chem. Phys. **55**, 1299 (1971).

[29] F. Rasetti, Über die Rotations-Ramanspektren von Sctickstoff und Sauerstoff, Z. Phys. **61**, 598 (1930).

[30] H. Krüger, Über die anreicherung des N^{15} isotops und einige specktroskopische untersuchungen am N^{15}, Z. Phys. **111**, 467 (1939).

[31] R. W. Wood and G. H. Dieke, The nuclear spin of N^{15}, J. Chem. Phys. **6**, 908 (1938).

[32] A. J. Lorquet and J. C. Lorquet, Isotopic effects in accidental predissociation. The case of the $C^2\Sigma_u^+$ state of N_2^+, Chem. Phys. Lett. **26**, 138 (1974).

[33] S. R. Langhoff and C. W. Bauschlicher, Theoretical study of the first and second negative systems of N_2^+, J. Chem. Phys. **88**, 329 (1988).